Coherent probe-pump-based Brillouin sensor for centimeter-crack detection

Lufan Zou, Xiaoyi Bao, Yidun Wan, and Liang Chen

Fiber Optics Group, Department of Physics, University of Ottawa, 150 Louis Pasteur, Ottawa, Ontario K1N 6N5, Canada

Received July 8, 2004

We provide a theoretical explanation for a coherent probe-pump-based Brillouin sensor system that achieves centimeter spatial resolution with high-frequency resolution. It was recently discovered that, when a combination of cw and pulsed light (the probe beam) interacts with a cw laser (the pump beam), centimeter spatial resolution with high-frequency resolution can be achieved even though the probe-pulse duration is 1.5 ns [Opt. Lett. **29,** 1485 (2004)]. Our study reveals that the coherent portion inside the pulse length of these two interactions caused by the same phase is responsible for this behavior. It allows us to detect 1.5-cm outer-layer cracks on an optical ground-wire cable. © 2005 Optical Society of America

OCIS codes: 290.5830, 060.2370, 290.5900, 190.5890, 060.2310.

Detecting cracks in structures is a major challenge: Only a specialized tool can find the target, and the highest resolution is required to take its measurement.[1] Moreover, detection strategies tend to be developed with specific structural materials in mind. Widely available and successful techniques used on steel structures cannot be applied to polyvinyl chloride or concrete structures because of the electrical nonconductance of the material. Recently, fiber Bragg grating (FBG) sensors were applied to the detection of cracks in carbon-fiber-reinforced plastic with a strain resolution of 1 $\mu\varepsilon$.[2] Obviously this FBG technology is material independent. In its basic form a typical FBG has a gauge of approximately 5 mm.[3] Thus it works as a point sensor. Since the crack locations in a structure are unknown *a priori*, conventional point sensors are not effective in crack sensing.

Sensors based on Brillouin scattering provide an excellent opportunity for structural-health monitoring of civil-engineering structures[4] by allowing measurements to be taken along the fiber rather than at discrete points. One class of Brillouin-based sensors is based on the Brillouin loss technique,[5] in which two counterpropagating laser beams, a pulsed Stokes beam and a cw pump beam, exchange energy through an induced acoustic field. Although the spatial resolution can be improved by use of short pulses, the loss spectrum broadens and the amplitude of the spectrum decreases as the pulse width decreases below the phonon lifetime of 10 ns, which makes it difficult to measure the Brillouin frequency shift accurately and results in a 1-m spatial resolution limitation.[6] Recently, we discovered that, when a combination of cw and pulsed light as the probe beam interacted with a cw laser as the pump beam, the uncertainty of $\delta\nu_B = 0.23$ MHz in measuring the Brillouin frequency, a signal-to-noise ratio (SNR) of 34 dB for 15-$\mu\varepsilon$ accuracy, and a temperature resolution of 1.3 °C were achieved with 1.5-ns (equivalent to 15-cm spatial resolution) pulses.[7] In this Letter we present a theoretical explanation for the results shown in Ref. 7 and demonstrate that our setup is able to detect centimeter cracks.

Considering a Mach–Zehnder modulator with two arms, as shown in Fig. 1, to convert a cw laser beam into a pulsed laser beam with a controllable pulse width, the output electrical field can be generally represented by

$$E_{\text{out}} = \frac{\sqrt{2}}{2}[A_1 \cos(\omega t + \varphi_1) + A_2 \cos(\omega t + \varphi_2)], \quad (1)$$

where ω is the frequency of the input cw laser, A_1 and A_2 represent the electric field amplitudes in the two arms, and φ_1 and φ_2 represent the respective optical phase delays. The output intensity is

$$I_{\text{out}} = |E_{\text{out}}|^2 = \frac{1}{2}\{I_1 + I_2 + 2(I_1 I_2)^{1/2}\cos[\varphi(t)]\}, \quad (2)$$

where I_1 and I_2 represent the intensities in the two arms, and the phase difference between the two arms $\varphi(t)(= \varphi_1 - \varphi_2)$ is time dependent through an applied ac voltage. If the optical waves are in phase $[\varphi(t) = 0]$ after propagating through the two arms, a maximum intensity output is reached whereas, if the optical waves are out of phase $[\varphi(t) = \pi]$ after propagating through the two arms, they combine at inverse phase, and the output intensity is minimum. In practice, I_1 is not equal to I_2, and $\varphi(t)$ cannot be exactly equal to π. Thus the electro-optic modulator (EOM) always has a finite extinction ratio (ER) defined as $R_x = (I_{\text{out}})_{\max}/(I_{\text{out}})_{\min}$, and the pulsed laser generated by the EOM always contains a cw (dc) component, as shown in Fig. 1. Then Eq. (1) becomes

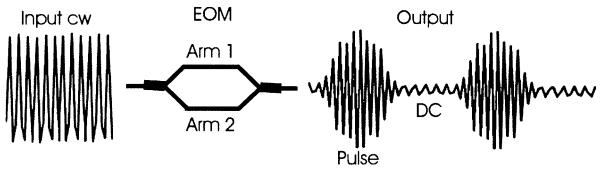

Fig. 1. Schematic of the electrical field before and after propagating through an EOM.

0146-9592/05/040370-03$15.00/0

$$E_{\text{out}} = \begin{cases} A_{\text{dc}} \cos(\omega t + \varphi_{\text{dc}}) & t < t_0 - \tau_p/2, t > t_0 + \tau_p/2 \\ A_{\text{pulse}} \cos(\omega t + \varphi_{\text{pulse}}) & t_0 - \tau_p/2 \le t \le t_0 + \tau_p/2 \end{cases}, \quad (3)$$

where A_{dc} is the electrical amplitude of the dc component. The electrical amplitude of the pulsed portion A_{pulse} can be divided into two parts: a_{dc}, the amplitude equal to the dc component A_{dc} and a_{pulse}, a super-Gaussian pulse centered at t_0 with a width of τ_p, $\exp\{-(\ln 2/2)[(t - t_0)/(\tau_p/2)]^m\}$, and yields

$$E_{\text{out}} = \begin{cases} A_{\text{dc}} \cos(\omega t + \varphi_{\text{dc}}) & t < t_0 - \tau_p/2, t > t_0 + \tau_p/2 \\ a_{\text{dc}} \cos(\omega t + \varphi_{\text{pulse}}) + a_{\text{pulse}} \cos(\omega t + \varphi_{\text{pulse}}) & t_0 - \tau_p/2 \le t \le t_0 + \tau_p/2 \end{cases}, \quad (4a)$$

or

$$E_{\text{out}} = \begin{cases} A_{\text{dc}} \cos(\omega t + \varphi_{\text{dc}}) + a_{\text{dc}} \cos(\omega t + \varphi_{\text{pulse}}) \\ a_{\text{pulse}} \cos(\omega t + \varphi_{\text{pulse}}) \end{cases}. \quad (4b)$$

Consequently, the Brillouin interaction of the pump and Stokes beams (i.e., E_{out}) in the fiber consists of both pump–dc and pump–pulse interactions. Note the Brillouin loss spectrum produced by the interaction of the first dc part [Eq. (4b)] with the pump has information about only the strain and (or) temperature along the test fiber, which has no spatial information. This is confirmed by the experimental result in the Brillouin peak from photonic crystal fiber (PCF) by looking at the region of single-mode fiber (SMF) in which SMF and PCF connect to each other,[7] as shown in Fig. 2(a). Since the PCF peak is 740 MHz from the SMF peak and the PCF peak intensity is six times higher than that of the SMF peak,[7] the two peaks could be easily discriminated even though we looked at the SMF region, but the PCF peak was very small. When the dc components were reduced by 5 dB, the PCF peak disappeared, but the SMF profile was still narrow with a high SNR, as shown in Fig. 2(b), which is attributed to the pump interacting with the super-Gaussian pulse and the second dc part of Eq. (4b). Because the electrical fields of the super-Gaussian pulse and the second dc part of Eq. (4b) have the same frequency and phase, they interact with the pump coherently. As a result, the Brillouin loss signal for this section is amplified coherently, and the Brillouin loss spectrum picks up only the local strain and (or) temperature information because of the narrow pulse width and localized phonon field. It is well known that a narrow pulse width yields high spatial resolution and a wide profile in the frequency domain that reduces the accuracy of Brillouin frequency analysis. However, if the pump–pulse and pump–dc [the second dc part of Eq. (4b)] interactions are coherent, the Brillouin loss signal is enhanced and the Brillouin loss profile is narrower than those of only pump–pulse interaction, as shown in Fig. 3, which is a numerical simulation based on Eq. (4b) and three coupled differential equations,[8] including the Brillouin interaction of the pump and the pulse (infinite ER) and the Brillouin interactions of the pump and the pulse coherently with the pump and the dc component (15 and 20 dB ER, respectively), which matches well with Lorentzian fits by FWHM of 46, 58, and 952 MHz for ER = 15 dB, 20 dB, and infinity, respectively. This numerical simulation agrees with experimental results, as shown in Fig. 4, which yields good Lorentzian fits too by the FWHM of 46 and 56 MHz for ER = 15 and 20 dB, respectively. However, if the phase of all the dc components [both dc portions in Eq. (4b)] is treated the same as that

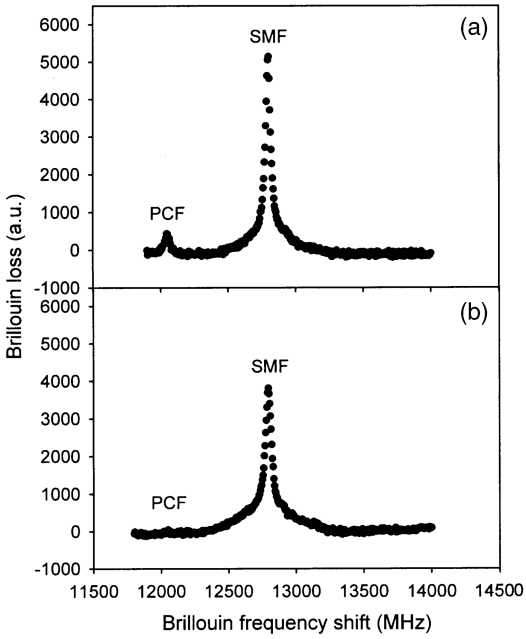

Fig. 2. Brillouin spectra when looking at the region of SMF. (a) Pump–dc interaction results in the appearance of a Brillouin peak from PCF. (b) Peak from PCF disappears when the dc portion is reduced by 5 dB.

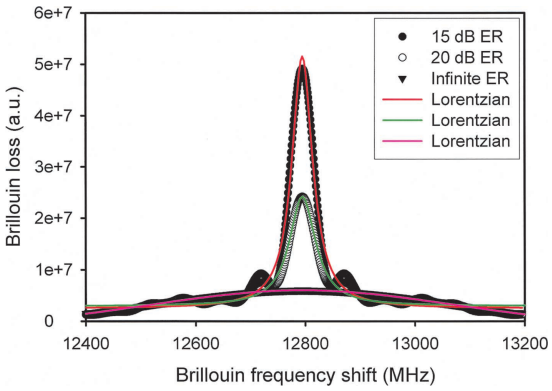

Fig. 3. Brillouin profiles of pump–pulse interaction and the pump and the pulse interacting coherently with the pump and the dc component.

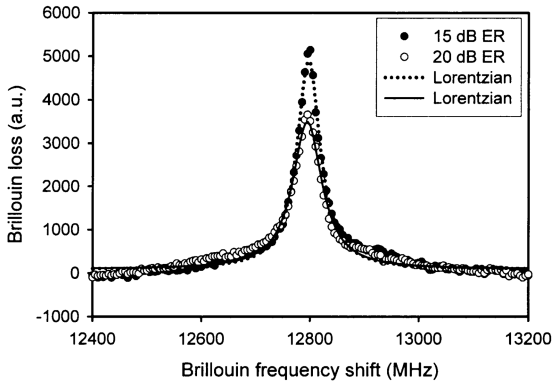

Fig. 4. Experimental Brillouin profiles, an enlargement of Fig. 2, which is coincident with the numerical simulation shown in Fig. 3.

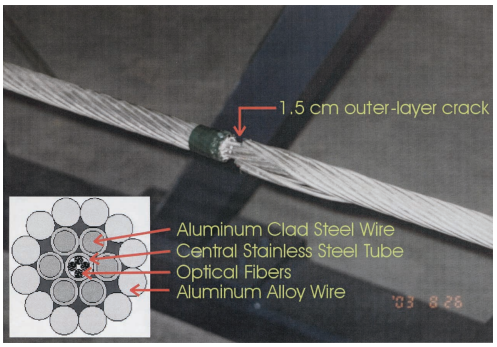

Fig. 5. 1.5-cm outer-layer crack on an OPGW cable. Inset, schematic of the OPGW cable.

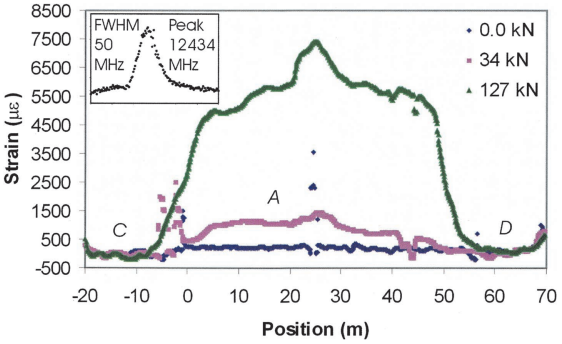

Fig. 6. Strain distributions along the OPGW cable.

of the pulse, the Brillouin spectrum will be broadened with a non-Lorentzian shape.[8] With an EOM being used as a pulse generator the phases of the dc components inside and outside the pulse length are different because of the applied dc voltage. They must be treated differently. Apparently, the coherent portion of pump–pulse and pump–dc interactions inside the pulse length makes a major contribution to the Brillouin profile. It provides localized information and enhances measurement accuracy as demonstrated in small-crack detection in an optical ground wire (OPGW) cable as shown in Fig. 5. One of 12 large-effective-area fibers located inside a central stainless-steel tube was used as a sensing fiber. A 1.5-cm-wide crack occurred in the outer layer of the OPGW cable. The OPGW cable in the test was 93 m long and included a stress region A (56 m, central part of 93 m) and two loose regions C and D, as indicated in Fig. 6, which displays strain distributions along the cable analyzed by our Brillouin fiber sensor with a 1.5-ns pulse. To make the cable straight, a force hereafter called 0.0 kN was applied on both sides of the cable, which resulted in 233 $\mu\varepsilon$ in region A compared with loose regions C and D on average. Strain vibrations around 0 and 56 m were caused by two chucks of a stress machine. The vibration of strain around 24 m was due to a strap hanging at this point on the cable. This vibration disappeared when the cable was stretched more. Although the holding areas of the chuck of the stress machine and the hanging strap were a few centimeters, our Brillouin fiber sensor could identify them. When the stress was increased to 34 kN, an outer-layer cut was made, and the strain distribution along the cable shows that a strain peak appeared in the crack region. The strain along the fiber decreases gradually from a high-strain area to a low-strain area since the optical fiber is a continuous medium. Because (1) each Brillouin spectrum was taken every 5 cm, (2) 1.5-ns pulses cover only 15 cm of fiber, and (3) Brillouin interaction picks up only the local strain information as discussed above and yields a high SNR profile (as shown in the inset of Fig. 6), the Brillouin frequencies were different for each 5 cm when closed to the crack region, so that a strain peak appears in the crack region.

In summary, the Brillouin interaction of Stokes and pump beams in the fiber includes both pump–dc and pump–pulse interactions in the probe-pump Brillouin sensor system. The dc component can be separated into two portions by their phases after propagating through the EOM. The dc part outside the pulse length interacting with the pump gathers information from all over the fibers and loses the spatial information, whereas the interaction of the pump with the dc component inside the phase length is coherent with the pump–pulse interaction, which amplifies the Brillouin signal significantly. It provides localized information about the strain and (or) temperature and enhances measurement accuracy, which allows the probe-pump-based Brillouin sensor to detect centimeter cracks.

References

1. H. Xiao and P. B. Nagy, J. Appl. Phys. **83,** 7453 (1998).
2. Y. Okabe, N. Tanaka, and N. Takeda, Smart Mater. Struct. **11,** 892 (2002).
3. W. L. Schulz, J. P. Conte, and E. Udd, Proc. SPIE **4330,** 56 (2001).
4. L. Zou, G. A. Ferrier, S. Afshar V., Q. Yu, L. Chen, and X. Bao, Appl. Opt. **43,** 1583 (2004).
5. X. Bao, D. J. Webb, and D. A. Jackson, Opt. Lett. **18,** 1561 (1993).
6. T. Horiguchi, K. Shimizu, T. Kurashima, M. Tateda, and Y. Koyamada, J. Lightwave Technol. **13,** 1296 (1995).
7. L. Zou, X. Bao, S. Afshar V., and L. Chen, Opt. Lett. **29,** 1485 (2004).
8. S. Afshar V., G. A. Ferrier, X. Bao, and L. Chen, Opt. Lett. **28,** 1418 (2003).